SF2A 2014
J. Ballet, F. Bournaud, F. Martins, R. Monier and C. Reylé (eds)

PHOTOMETRIC REDSHIFTS FOR THE NGVS

A. Raichoor[1], S. Mei[1,2], T. Erben[3], H. Hildebrandt[3], M. Huertas-Company[1,2], O. Ilbert[4], R. Licitra[1,2], N.M. Ball[5], S. Boissier[4], A. Boselli[4], Y.-T. Chen[6], P. Côté[5], J.-C. Cuillandre[7], P.A. Duc[8], P.R. Durrell[9], L. Ferrarese[5], P. Guhathakurta[10], S.D.J. Gwyn[5], J.J. Kavelaars[5], A. Lancon[11], C. Liu[12], L.A. MacArthur[5], M. Muller[10], R.P. Muñoz[13], E.W. Peng[14], T.H. Puzia[13], M. Sawicki[15], E. Toloba[10,16], L. Van Waerbeke[17], D. Woods[17] and H. Zhang[14,18]

Abstract. We present the photometric redshift catalog for the Next Generation Virgo Cluster Survey (NGVS), a 104 deg^2 optical imaging survey centered on the Virgo cluster in the u^*, g, r ,i, z bandpasses at point source depth of 25-26 ABmag. It already is the new optical reference survey for the study of the Virgo cluster, and will be also used for multiple ancillary programs. To obtain photometric redshifts, we perform accurate photometry, through the PSF-homogenization of our data. We then estimate the photometric redshifts using *Le Phare* and BPZ codes, adding a new prior extended down to $i_{AB} = 12.5$ mag. We assess the accuracy of our photometric redshifts as a function of magnitude and redshift using ∼80,000 spectroscopic redshifts from public surveys. For $i_{AB} < 23$ mag or $z_{\rm phot} < 1$ galaxies, we obtain photometric redshifts with $|bias| < 0.02$, a scatter increasing with magnitude (from 0.02 to 0.05), and less than 5% outliers.

Keywords: Galaxies: distances and redshifts – Galaxies: high-redshift – Galaxies: photometry techniques: photometric.

1 Introduction

Current large surveys (e.g., the Sloan Digital Sky Survey; SDSS; York et al. 2000) and future missions (e.g., such as EUCLID; Laureijs et al. 2011) open a new era for many field of astronomy, such as galaxy evolution and

[1] GEPI, Observatoire de Paris, CNRS, Université Paris Diderot, 61, Avenue de l'Observatoire 75014, Paris France
[2] Université Paris Denis Diderot, F-75205, Paris Cedex 13, France
[3] Argelander-Institut für Astronomie, University of Bonn, Auf dem Hügel 71, D-53121 Bonn, Germany
[4] Aix Marseille Université, CNRS, Laboratoire d'Astrophysique de Marseille, UMR 7326, F-13388 Marseille, France
[5] Herzberg Institute of Astrophysics, National Research Council of Canada, Victoria, BC, V9E 2E7, Canada
[6] Insitute of Astronomy and Astrophysics, Academia Sinica, P.O. Box 23-141, Taipei 106, Taiwan
[7] Canada–France–Hawaïi Telescope Corporation, Kamuela, HI 96743, USA
[8] Laboratoire AIM Paris-Saclay, CEA/IRFU/SAp, CNRS/INSU, Université Paris Diderot, F-91191 Gif-sur-Yvette Cedex, France
[9] Department of Physics and Astronomy, Youngstown State University, Youngstown, OH, USA
[10] UCO/Lick Observatory, Department of Astronomy and Astrophysics, University of California Santa Cruz, 1156 High Street, Santa Cruz, California 95064, USA
[11] Observatoire astronomique de Strasbourg, Université de Strasbourg, CNRS, UMR 7550, 11 rue de l'Université, F-67000 Strasbourg, France
[12] Center for Astronomy and Astrophysics, Department of Physics and Astronomy, Shanghai Jiao Tong University, 800 Dongchuan Road, Shanghai 200240, China
[13] Institute of Astrophysics, Pontificia Universidad Católica de Chile, Av. Vicuña Mackenna 4860, 7820436 Macul, Santiago, Chile
[14] Department of Astronomy, Peking University, Beijing 100871, China
[15] Department of Astronomy and Physics, St. Mary's University, Halifax, NS B3H 3C3, Canada
[16] Observatories of the Carnegie Institution for Science, 813 Santa Barbara Street, Pasadena, CA 91101, USA
[17] Department of Physics and Astronomy, University of British Columbia, 6224 Agricultural Road, Vancouver, B.C., V6T 1Z1, Canada
[18] Chinese Academy of Sciences South America Center for Astronomy, Camino El Observatorio #1515, Las Condes, Santiago, Chile

Table 1. Average characteristics of the NGVSLenS co-added data used in this study.

Filter	expos. time [ks]	$m_{\rm lim}^{\dagger}$ [AB mag]	seeing ["]
$u^*(u.MP9301)$	6.3	25.60 ± 0.16	0.83 ± 0.07
$g(g.MP9401)$	3.5	25.73 ± 0.13	0.77 ± 0.08
$r(r.MP9601)$	2.6	$24.68 \pm 0.50^{\star}$	0.74 ± 0.14
$i(i.MP9702)$	2.3	24.41 ± 0.13	0.52 ± 0.04
$z(z.MP9801)$	4.6	23.62 ± 0.16	0.70 ± 0.08

†: $m_{\rm lim}$ is the 5σ detection limit in a 2" aperture.

*: for the r-band, the minimum and maximum values for $m_{\rm lim}$ are 23.56 and 25.52, respectively.

cosmology, with access to homogeneous measurements of a multitude of fundamental galaxy properties. In this context, a crucial quantity is the galaxy redshift: spectroscopic redshifts (spec-z's) being observationally too costly for 10^6-10^8 objects, photometric redshifts (photo-z's) allow consistent measurement of redshifts for large numbers of galaxies, including relatively faint ones. The main limitations to estimate accurate photo-z's are the wavelength coverage of key spectral features (e.g., the Lyman-break and the 4,000 Å/Balmer break), and the quality and homogeneity of the photometry.

We present here the estimation of photo-z's for the Next Generation Virgo Cluster Survey (NGVS; Ferrarese et al. 2012). The NGVS is a comprehensive optical imaging survey of the Virgo cluster, from its core to its virial radius – covering a total area of 104 deg^2 – in the Canada-France-Hawaii Telescope (CFHT) u^*griz bandpasses. Currently, ∼70% of the NGVSLenS has not been imaged yet with the r-band. The NGVS will serve as the optical reference survey over the Virgo cluster, and will leverage the numerous other surveys targeting Virgo at shorter and longer wavelengths.

The results presented here are detailed in Raichoor et al. (2014).

2 NGVSLenS data and photometric catalogs

For this analysis, we use a NGVS dataset whose reduction is optimized for *background-science* (e.g., detection of high-redshift galaxy cluster candidates, Licitra et al., *in preparation*; strong and weak lensing studies, Gavazzi et al., *in preparation*): we label this dataset NGVSLenS.

To process the NGVS data for *background-science* applications, we use the algorithms and processing pipelines (THELI) developed within the Canada-France-Hawaii-Telescope Lensing Survey (CFHTLenS; see Heymans et al. 2012; Hildebrandt et al. 2012; Erben et al. 2013, and `http://cfhtlens.org`), a survey originated from the Wide component of the Canada-France-Hawaii-Telescope Legacy Survey (CFHTLS; Gwyn 2012) which was also obtained with MegaCam. In addition, the survey characteristics and the observing strategies of CFHTLS and NGVS are very similar. This allowed for a direct transfer of our CFHTLS expertise to the NGVS. The NGVSLenS dataset average characteristics are summarized in Table 1.

As studied in detailed in Hildebrandt et al. (2012), a requirement to estimate precise photo-z's is accurate photometry, in particular high precision color measurements. To do so, we implement the following procedure (*global* mode of Hildebrandt et al. 2012): the i-band, which has the best seeing (0.52" ± 0.04"), is used to detect objects and estimate their total magnitude; then, for each field, all images are first homogenized to the same PSF and then used to estimate accurate colors. In addition, we pay special attention to the photometric error estimation, to overcome a possible underestimation due to noise correlation introduced by image resampling.

3 Photometric redshift estimation

With the photometric catalogs described in the previous section in hand, we are able to estimate the photo-z's. We use two template-based codes to estimate photo-z's: *Le Phare* (Arnouts et al. 2002; Ilbert et al. 2006) and BPZ (Benítez 2000). For both codes, we use the recalibrated template set of Capak et al. (2004), which is built from the four Coleman et al. (1980) observed galaxy spectra (El, Sbc, Scd, Im), with two additional observed starburst templates from Kinney et al. (1996).

Le Phare and BPZ run in a similar way using a Bayesian approach. Both codes were designed for high redshift studies: they use similar priors for $i > 20$ mag galaxies, built with observed data. We use the SDSS Galaxy Main Sample spectroscopic survey (Strauss et al. 2002) to establish the prior for $12.5 < i \leq 17$ mag galaxies, and extrapolate the prior for $17 < i < 20$ mag galaxies.

4 Photometric redshift accuracy

To measure the accuracy of our photo-z's, we use a large sample of galaxy spec-z's (83.3×10^3 galaxies).

Our NGVSLenS spectroscopic sample (26.1×10^3 galaxies) is a compilation of several spectroscopic surveys having different target selections (SDSS: Eisenstein et al. 2001; Strauss et al. 2002; Dawson et al. 2013; spectroscopic programs targeting candidate globular clusters or UCDs: Peng et al., *in preparation*, Zhang et al., *submitted*; Zhang et al., *in preparation*, and spec-z's from the VDGC survey: Guhathakurta et al., *in preparation*). It is rather shallow ($z \leq 0.8$) and highly biased at $z \geq 0.3$ towards luminous red galaxies (LRGs), from the SDSS.

In order to assess the quality of our photometric redshifts up to $z < 1.5$, we use the CFHTLenS data, which are covered by deep and intensive spectroscopic surveys (DEEP2/EGS: Davis et al. 2003; Newman et al. 2013; VIPERS: Guzzo et al. 2013; F02 and F22 fields of the VVDS: Le Fèvre et al. 2013). Our CFHTLenS spectroscopic sample includes 57.2×10^3 spec-z's and spreads over $\sim$42 deg^2. Starting from the CFHTLenS THELI coadded-images, we re-estimate for the CFHTLenS the photometry and photo-z's, with the THELI pipeline including our introduced modifications.

By comparing with the NGVSLenS photometric objects, our combined spectroscopic sample spans with high coverage the color-color space for $i < 23$ mag objects, and satisfactorily covers the $23 < i < 24$ mag objects (the regions within the 68% contours are well populated by our spectroscopic sample).

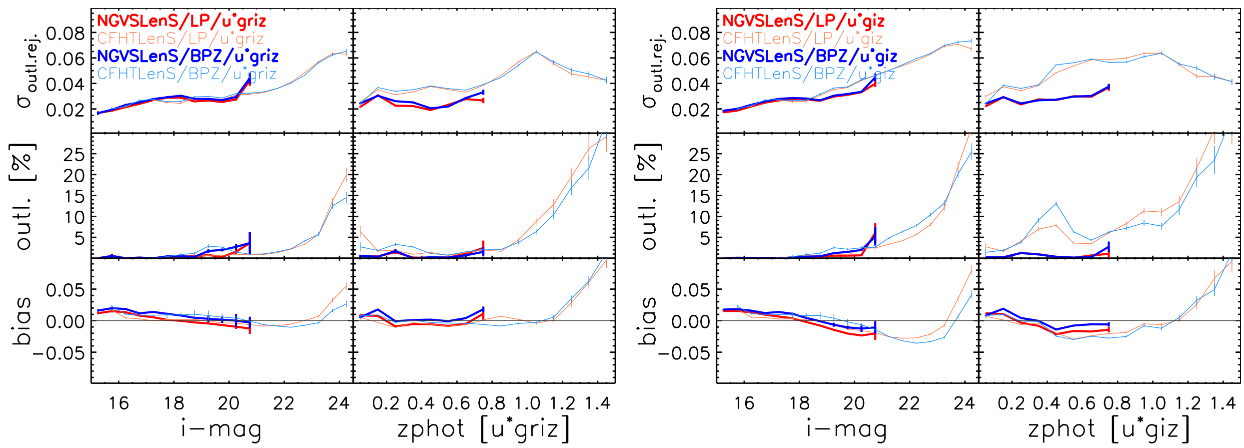

Fig. 1. Left: Statistics for photo-z's estimated with u^*griz bands as a function of magnitude (*left panel*) and redshift (*right panel*). Photo-z's estimated with *Le Phare* are in red and those estimated with BPZ are in blue. Dark thick lines represent the NGVSLenS spectroscopic sample (low redshift); light thin lines represent the CFHTLenS spectroscopic sample (high redshift). We report quantities only for the bins where we have more than 50 galaxies. Error bars are calculated assuming a Poissonian distribution. **Right**: same, but for photo-z's estimated with u^*giz bands.

In Figure 1, we quantify, as a function of magnitude and redshift, the accuracy of our photo-z's when they are estimated with the u^*griz-bands (left figure) or with the u^*giz-bands (right figure). For each object in our spectroscopic sample, we calculate $\Delta z = \frac{z_{\rm phot} - z_{\rm spec}}{1 + z_{\rm spec}}$ and classify it as an outlier if $|\Delta z| > 0.15$. For each considered sample, we report *bias*: the median value of Δz; *outl.*: the percentage of outliers; and $\sigma_{\rm outl.rej.}$: the standard deviation of Δz when outliers have been excluded.

When the photo-z's are estimated with the u^*griz-bands (*left* figure), we observe that the two codes and the two datasets (NGVSLenS and CFHTLenS) provide consistent behavior over our tested ranges in magnitude or photo-z. The only difference between the two datasets is in the $0.3 < z_{\rm phot} < 0.6$ range for the $\sigma_{\rm outl.rej.}$: the smaller $\sigma_{\rm outl.rej.}$ for the NGVSLenS sample is a direct consequence being of our NGVSLenS spectroscopic sample in this redshift range is highly biased towards LRGs. Overall, the quality of our photo-z's decreases with increasing magnitude or redshift: the *bias* becomes significant (> 0.02) for faint ($i > 23$ mag) or high-z ($z > 1.2$) objects, and the $\sigma_{\rm outl.rej.}$ goes from $\sim$0.02 for bright/low-z objects to $\sim$0.06 for faint/high-z objects. For $z_{\rm phot} > 1.2$, our optical data do not bracket the 4,000 Å break, and the photo-z's are less reliable.

When the photo-z's are estimated with the u^*giz-bands (*right* figure), our photo-z's are less accurate in the $0.3 < z_{\rm phot} < 0.8$ range, where the r-band filter is essential to constrain the 4,000 Å break. In this redshift interval, we have a $-0.05 < bias < -0.02$, a $\sigma_{outl.rej} \sim 0.06$ and an outlier rate that peaks at 10-15%. This effect is less pronounced for our NGVSLenS spectroscopic sample because it is highly biased towards LRGs: the prior – more peaked and at lower redshift than for average galaxies at similar redshift – helps to obtain fewer false values for the posterior.

In addition, we also make an analysis of the angular correlation function $w(\theta)$, to internally assess the quality of our photo-z's using the whole NGVSLenS sample with $i \leq 23$ mag and $0.1 \leq z_{\rm phot} \leq 1.2$.

5 Conclusion

We estimated the photo-z's for the 104 deg^2 of the NGVS. Using a robust spec-z sample (83.3×10^3 galaxies), we estimated our photo-z's properties for $i_{AB} < 24.5$ or $z_{\rm phot} < 1.4$, as a function of magnitude and redshift. The NGVSLenS catalogs will be public on June, 1st 2015 on the NGVS website*. Before that date, please contact us if you would like to use them †.

The French authors acknowledge the support of the French Agence Nationale de la Recherche (ANR) under the reference ANR10-BLANC-0506-01-Projet VIRAGE. SM acknowledges financial support from the Institut Universitaire de France (IUF). H.H. is supported by the DFG Emmy Noether grant Hi 1495/2-1. C.L. acknowledges support from the National Natural Science Foundation of China (Grant No. 11203017, 11125313 and 10973028). R.P.M. acknowledges support from FONDECYT Postdoctoral Fellowship Project No. 3130750. E.W.P. acknowledges support from the National Natural Science Foundation of China under Grant No. 11173003, and from the Strategic Priority Research Program, "The Emergence of Cosmological Structures", of the Chinese Academy of Sciences, Grant No. XDB09000105. T.H.P. acknowledges support from FONDECYT Regular Grant (No. 1121005) and BASAL Center for Astrophysics and Associated Technologies (PFB-06). H.Z. acknowledges support from the China–CONICYT Post-doctoral Fellowship, administered by the Chinese Academy of Sciences South America Center for Astronomy (CASSACA).

References

Arnouts, S., Moscardini, L., Vanzella, E., et al. 2002, MNRAS, 329, 355
Benítez, N. 2000, ApJ, 536, 571
Capak, P., Cowie, L. L., Hu, E. M., et al. 2004, AJ, 127, 180
Coleman, G. D., Wu, C.-C., & Weedman, D. W. 1980, ApJS, 43, 393
Davis, M., Faber, S. M., Newman, J. A., et al. 2003, Proc.SPIE Int.Soc.Opt.Eng., 4834, 161
Dawson, K. S., Schlegel, D. J., Ahn, C. P., et al. 2013, AJ, 145, 10
Eisenstein, D. J., Annis, J., Gunn, J. E., et al. 2001, AJ, 122, 2267
Erben, T., Hildebrandt, H., Miller, L., et al. 2013, MNRAS
Ferrarese, L., Côté, P., Cuillandre, J.-C., et al. 2012, ApJS, 200, 4
Guzzo, L., Scodeggio, M., Garilli, B., et al. 2013
Gwyn, S. D. J. 2012, AJ, 143, 38
Heymans, C., Van Waerbeke, L., Miller, L., et al. 2012, MNRAS, 427, 146
Hildebrandt, H., Erben, T., Kuijken, K., et al. 2012, MNRAS, 421, 2355
Ilbert, O., Arnouts, S., McCracken, H. J., et al. 2006, A&A, 457, 841
Kinney, A. L., Calzetti, D., Bohlin, R. C., et al. 1996, ApJ, 467, 38
Laureijs, R., Amiaux, J., Arduini, S., et al. 2011, ArXiv e-prints
Le Fèvre, O., Cassata, P., Cucciati, O., et al. 2013, A&A, 559, A14
Newman, J. A., Cooper, M. C., Davis, M., et al. 2013, ApJS, 208, 5
Raichoor, A., Mei, S., Erben, T., et al. 2014, ApJ, in press (arxiv: 1410.2276)
Strauss, M. A., Weinberg, D. H., Lupton, R. H., et al. 2002, AJ, 124, 1810
York, D. G., Adelman, J., Anderson, Jr., J. E., et al. 2000, AJ, 120, 1579

*https://www.astrosci.ca/NGVS/The_Next_Generation_Virgo_Cluster_Survey/Home.html
†simona.mei@obspm.fr